

AD \_\_\_\_\_

Award Number: DAMD17-99-1-9316

TITLE: Monochromatic Mammographic Imaging Using X-ray  
Polycapillary Optics

PRINCIPAL INVESTIGATOR: Francisca Sugiro, Ph.D.

CONTRACTING ORGANIZATION: University of Albany, SUNY  
Albany, New York 12222

REPORT DATE: June 2002

TYPE OF REPORT: Annual Summary

PREPARED FOR: U.S. Army Medical Research and Materiel Command  
Fort Detrick, Maryland 21702-5012

DISTRIBUTION STATEMENT: Approved for Public Release;  
Distribution Unlimited

The views, opinions and/or findings contained in this report are those of the author(s) and should not be construed as an official Department of the Army position, policy or decision unless so designated by other documentation.

113 0 11

**REPORT DOCUMENTATION PAGE**Form Approved  
OMB No. 074-0188

Public reporting burden for this collection of information is estimated to average 1 hour per response, including the time for reviewing instructions, searching existing data sources, gathering and maintaining the data needed, and completing and reviewing this collection of information. Send comments regarding this burden estimate or any other aspect of this collection of information, including suggestions for reducing this burden to Washington Headquarters Services, Directorate for Information Operations and Reports, 1215 Jefferson Davis Highway, Suite 1204, Arlington, VA 22202-4302, and to the Office of Management and Budget, Paperwork Reduction Project (0704-0188), Washington, DC 20503

<b>1. AGENCY USE ONLY (Leave blank)</b>		<b>2. REPORT DATE</b> June 2002	<b>3. REPORT TYPE AND DATES COVERED</b> Annual Summary (1 Jun 99 - 31 May 02)	
<b>4. TITLE AND SUBTITLE</b> Monochromatic Mammographic Imaging Using X-ray Polycapillary Optics			<b>5. FUNDING NUMBERS</b> DAMD17-99-1-9316	
<b>6. AUTHOR(S)</b> Francisca Sugiro, Ph.D.				
<b>7. PERFORMING ORGANIZATION NAME(S) AND ADDRESS(ES)</b> University of Albany, SUNY Albany, New York 12222  E-Mail: Fs5699@csc.albany.edu			<b>8. PERFORMING ORGANIZATION REPORT NUMBER</b>	
<b>9. SPONSORING / MONITORING AGENCY NAME(S) AND ADDRESS(ES)</b> U.S. Army Medical Research and Materiel Command Fort Detrick, Maryland 21702-5012			<b>10. SPONSORING / MONITORING AGENCY REPORT NUMBER</b>	
<b>11. SUPPLEMENTARY NOTES</b> report contains color				
<b>12a. DISTRIBUTION / AVAILABILITY STATEMENT</b> Approved for Public Release; Distribution Unlimited				<b>12b. DISTRIBUTION CODE</b>
<b>13. Abstract (Maximum 200 Words) (abstract should contain no proprietary or confidential information)</b> Monochromatic imaging is typically done with synchrotron sources. These sources are expensive and not practical for clinical settings. However, conventional laboratory sources normally have insufficient intensity. Polycapillary x-ray optics can be used to efficiently produce an intense parallel beam, which can be diffracted from a crystal to create monochromatic radiation. Monochromatic parallel beam imaging produces high subject contrast, high resolution, and low patient dose. Contrast, resolution, and intensity measurements were performed with both high and low angular acceptance crystals. Testing was first done at 8 keV with an intense copper rotating anode source. Preliminary 17.5 keV measurements were then made with a molybdenum source. At 8 keV, contrast enhancement was a factor of five relative to the polychromatic case, in good agreement with theoretical values. At 17.5 keV, monochromatic subject contrast was a factor of two times greater than the conventional polychromatic contrast. The measured angular resolution with a silicon crystal is 0.6 mrad at 8 keV, and 0.2 - 0.3 mrad at 17.5 keV. For a 50-mm thick patient, this angle corresponds to 50 lp/mm with an ideal detector. The use of polychromatic collimating optics allow monochromatic mammographic imaging measurements with a conventional x-ray source in a practical clinical setting.				
<b>14. SUBJECT TERMS</b> polycapillary optics, monochromatic imaging, x-ray mammography, breast cancer			<b>15. NUMBER OF PAGES</b> 14	
			<b>16. PRICE CODE</b>	
<b>17. SECURITY CLASSIFICATION OF REPORT</b> Unclassified	<b>18. SECURITY CLASSIFICATION OF THIS PAGE</b> Unclassified	<b>19. SECURITY CLASSIFICATION OF ABSTRACT</b> Unclassified	<b>20. LIMITATION OF ABSTRACT</b> Unlimited	

20021113 011

## Table of Contents

Cover.....	1
SF 298.....	2
Body.....	4
Key Research Accomplishments.....	11
Reportable Outcomes.....	11
Conclusions.....	13
References.....	14
Appendices.....	N/A

**Body:**

Monochromatic imaging involves a collimating optic, which makes the x-ray radiation parallel, and a diffracting crystal, which makes the beam monochromatic (a single energy wavelength).

**Objective 1: Laboratory measurements using an existing prototype optic**

**Objective 2: Verifying experimental results using computer simulations**

The characterizations of this optic have been addressed in first and second annual reports. Both objectives give the candidate exposure to experimental set-up of the x-ray sources, the optics, and the detectors. Aligning the optic with motion controllers and actuators becomes a learned skill. The solid-state detectors are hooked up with multi-channel analyzers and amplifiers, which gives the candidate some exposure to some practical electronic knowledge. The computer simulations give a good training for the computer software and learning QUICK BASIC language.

**Objective 3:**

**Testing the optimal optic/crystal combination.**

This objective was on going from last annual report. Both objectives 3 and 4 give the candidate the opportunity to attend three meetings in the year 2000: the EOH meeting, the Chicago World Congress for Medical Physicists and Biomedical Engineers, and the annual SPIE conference. In these meetings, the candidate learned how to present posters, give talks, and write papers. In the year 2001, the candidate went to the Denver X-ray Conference for a poster session. Unique learning experiences included technical writing, public speaking, and arranging information in a poster format in Microsoft Power Point. The SPIE and the Denver conference resulted in paper publications. By attending these conferences, the candidate learned the state of the art research talks in other research institutions.

In the laboratory, the candidate learned taking the x-ray rotating anode apart and cleaning the anode. She also learned how to measure resolution with a tantalum knife-edge and to convert the measurement into line pairs/mm, which is the normal usage for resolution in medical imaging.

**A) Total Photon Flux:**

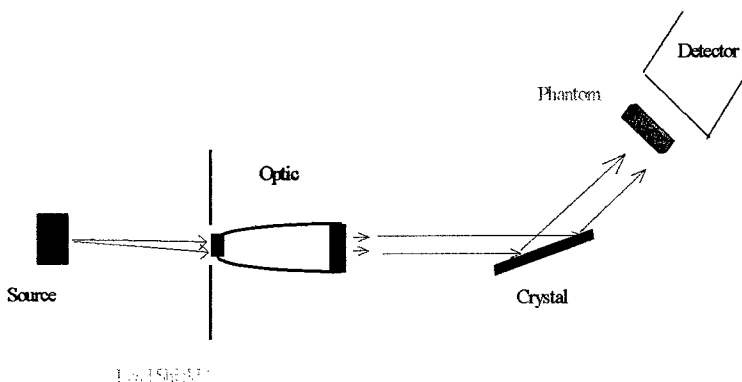


Figure 1. Monochromatic imaging set-up.

Monochromatic imaging uses an optic and crystal. The set-up is shown in figure 1. To measure the flux, the detector was used without the optic and crystal, with the optic only and with optic/crystal combination. All measurements were taken without the phantom. The counts were taken with a 6.5 – 19.5 keV window NaI detector with and without optic.

Without the optic/crystal combination, the theoretical calculation for a copper source operating at 20 kVp and 10 mA is

$$F = \epsilon_{\text{char}} \left( \frac{10 \times 10^{-3} \text{ C}}{\text{s}} \right) \left( \frac{1 \text{ electron}}{1.6 \times 10^{-19} \text{ C}} \right) \quad (1)$$

where  $\epsilon_{\text{char}}$  is the efficiency of the characteristic line. The characteristic flux and bremsstrahlung is  $7.0 \times 10^{13}$  photons/second.

The experimental value was taken with an 8 mm by 8 mm hole at a distance  $d$  of 263 mm from the source. Aluminum filters were inserted to prevent dead-time. The measured intensity is

$$I = \frac{C(4\pi d^2)}{\text{area}_{\text{hole}}}, \quad (2)$$

where  $d$  is the diameter of the pinhole and  $C$  is the source output. The computed source output from the measurement was  $3.9 \times 10^{10} \pm 3.2 \times 10^{10}$  photons/second taking the filters into account.

An exposure of 300 mAs was expected for an exposure time of 30 seconds with 10 mA current. However, the x rays generated by the rotating anode were much less than expected. The experimental value differs by a factor 1000 from the theoretical one. Therefore, the exposure may have been only 0.3 mAs.

The expected flux with the optic is

$$F_{\text{optic}} = (F)(\Omega_{\text{optic}})(T_{\text{optic}}), \quad (3)$$

where  $F$  is the experimental flux before the optic,  $\Omega_{\text{optic}}$  is the solid angle of the optic, and  $T_{\text{optic}}$  is the optic transmission (39 %). The flux after the optic was calculated to be  $1.2 \times 10^6$  photons/second.

The experimental flux was measured with an area hole of 8 mm by 8 mm, which was approximately the size of the input of the beam before the optic at approximately 250 mm from the source. The experimental count was  $5.1 \times 10^5 \pm 4 \times 10^5$  photons/second. The optic data differs from the theoretical values due to fluctuations caused by the instability of the anode and variation in intensity. Variations also occurred if the optic was not always well-aligned.

The expected flux after optic/crystal combination was

$$F_{\text{crystal}} = (F_{\text{optic}})(\eta)(R_{\text{crystal}}) \quad (4)$$

where  $F_{\text{optic}}$  is the experimental flux through the optic,  $\eta$  is the coefficient of the crystal and  $R_{\text{crystal}}$  is the reflectivity of the crystal. The intensity reflected by the crystal is  $\eta$  multiplied by the reflectivity,  $R_{\text{crystal}}$ , of the crystal, which was  $R_{\text{crystal}} = 1$ , for silicon and  $R_{\text{crystal}} = 0.2$  for graphite. For mica a fit to the data gave  $R_{\text{crystal}} = 0.1$ . Table 1 shows the comparison of the counts after the optic and crystal. The counts after the crystal in theory are in approximately in the right order of magnitude.

Crystal	Efficiency $\eta$	$R_{\text{crystal}}$	Flux Data	Theory
Silicon	0.005	1	$2,000 \pm 1,600$	2,550
Mica	0.097	0.1	$4,000 \pm 3,300$	4,950
Graphite	1.0	0.2	$104,000 \pm 86,000$	102,000

Table 1. The flux comparison between data and theory with the copper rotating anode source

standard deviation over the mean for each measurement taken with a 2.1-mm diameter pinhole scanned across the optic's output. The non-uniformity is the difference between the STD/mean

## B) Beam Uniformity

The uniformity of the beam is defined as the

and the Poisson statistics. The count is uniform before, after the optic, and after the optic/crystal combination. After the optic, the only non-uniformity arose from the inter-fiber spacing. The non-uniformity is about 15.1 % over all energies.

### C) Resolution

The motivation for examining angular divergence in the system is that the divergence of the x-ray beam after the optic causes blurring in the image of small features at the entrance side of the thick phantom. Because the output beam of the optic is not completely parallel, i.e. the resolution is

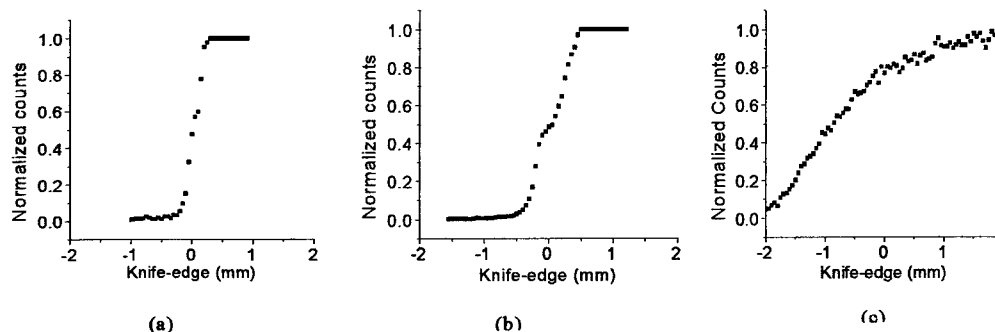


Figure 2. Knife-edge resolution profiles obtained with silicon (a), mica (b) and graphite (c) crystals.

affected. To maintain good spatial resolution, angular divergence must be controlled. The exit divergence from capillary optics is measured by rotating a high quality crystal (usually silicon) in the beam and measuring the angular width of the characteristic line of the Bragg peak.

For the narrowest bandwidth crystal, silicon, the entire rocking curve width is due to the optic divergence. For mica, the width is a combination of the divergence and the crystal width. For graphite, the crystal dominates. The widths are summarized in table 2.

Crystal:	Company's specification $\alpha$ (m rad):	Measured rocking curve width (m rad):	Angular width of knife-edge image (m rad):	$\sigma$ , Theory with 50 $\mu$ m pixel detector (m rad):	$\sigma$ , Theory with an ideal detector (m rad):	Resultant resolution for 50-mm thick patient with ideal detector (lp/mm)
Silicon	0.02	$4.0 \pm 0.1$	$0.54 \pm 0.20$	0.59	0.57	18
Mica	0.4 - 0.6	$4.4 \pm 0.2$	$0.78 \pm 0.20$	0.56 - 0.71	0.53 - 0.69	14
Graphite	35 - 87	$42.5 \pm 1.1$	$6.5 \pm 0.5$	4.5	4.5	2

Table 2. Rocking curves and resolution measurements using three different crystals.

A knife-edge made of tantalum was placed after the monochromatic parallel beam. An image plate was placed 300 mm from the knife-edge to achieve an angular resolution of  $50 \mu\text{m}/300 \text{ mm} = 0.167 \text{ mrad}$  with the 50- $\mu\text{m}$  resolution of the Fuji plate detector.

A perfect crystal and parallel monochromatic input beam, with a perfect detector would result in an ideally sharp knife-edge. For a crystal with a large bandwidth, such as graphite, the angular width is determined by the optic divergence, since the crystal can accommodate the full range of angles output from the optic. For a crystal with a bandwidth narrower than the optic divergence, a

monochromatic beam would give a width equal to the crystal bandwidth. The 4-eV energy width of the  $K_{\alpha 2}$  emission line produces an additional angular spread of

$$\sigma_E \equiv \tan \theta_0 \frac{\sigma_{K_{\alpha 2}}}{E_{K_{\alpha 2}}} \approx 0.34 \text{ mrad} \quad (5)$$

where  $\theta_0$  is the  $K_{\alpha 2}$  Bragg angle ( $34.675^\circ$ ), for copper  $\sigma_{K_{\alpha 2}}$  is 4 eV and  $E_{K_{\alpha 2}}$  is 8027.83 eV.<sup>1,2</sup>

Combining the effects of the crystal, optic divergence, and energy spread, the angular distribution of intensity off the crystal should be given by a Gaussian distribution,

$$I(\Delta\theta) = \iint I(\phi) I(E(\beta)) p(\beta) \delta(\Delta\theta - \phi + 2\beta) d\phi dE, \quad (6)$$

where  $\Delta\theta$  is the deviation of the output angle from the normal Bragg angle,  $I(\phi)$  is the angular distribution from the optic, assumed to be a Gaussian of width  $\sigma_{\text{optic}}$ ,  $I(E)$  is the spectral distribution of the  $K_{\alpha 2}$  line, also assumed Gaussian of width  $\sigma_E$ ,  $E(\beta)$  is the relationship between angles and energies given by Bragg's law, and  $p(\beta)$  is the probability distribution of the planes at angle  $\beta$  from the surface of the crystal, which has a width  $\alpha$  given by the crystal bandwidth.

Making the appropriate substitutions, and solving the integral analytically,

$$I(\Delta\theta) = I_0 \int e^{-\frac{\phi^2}{\sigma_{\text{optic}}^2}} e^{-\frac{(\phi + \Delta\theta)^2}{4\sigma_E^2}} e^{-\frac{(\phi - \Delta\theta)^2}{4\alpha^2}} d\phi \quad (7)$$

the output width is then

$$\sigma = \sqrt{\frac{4\sigma_E^2 \cdot \alpha^2 + \sigma_E^2 \cdot \sigma_{\text{optic}}^2 + \sigma_{\text{optic}}^2 \cdot \alpha^2}{\alpha^2 + \sigma_{\text{optic}}^2 + \sigma_E^2}} \quad (8)$$

The output width is additionally broadened by the detector resolution, which is of 0.167 mrad. The experimental angular resolutions, which are taken as the widths of the knife-edge profiles, are shown in table 2. The values agree fairly well with the calculated resolutions, for which the detector broadening in the knife-edge measurement has been added in quadrature as  $\sqrt{(0.569^2 + 0.167^2)} = 0.59$  mrad for silicon. Since the crystal bandwidth for graphite is very wide, the energy is taken as the middle ground between the  $K_{\alpha 1}$  and  $K_{\alpha 2}$  for calculating the output width.

The theoretical angular resolution from the optic/crystal system with an ideal detector and the silicon crystal would give a spatial resolution for an object on the front side of a 50-mm thick patient of 18 lp/mm for the  $K_{\alpha 1}$  peak. The  $K_{\alpha 2}$  peak gives 23 lp/mm, but would not be as intense.

#### Objective 4: Measure scatter fraction and contrast of mammographic phantoms

In this objective, the candidate learned how to design a contrast phantom and how to measure contrast. She also learned how to program in mathcad and quick basic to compute the theoretical contrast.

##### A) Scatter Fraction

When this project was initiated, the existing optic was a 30 mm by 30 mm wide output. However, the focal length of this optic, which had been designed for 8 keV, was too short to have good transmission at 20 keV. After this project was funded, another optic with a 10 mm by 10 mm output seemed to be a better optic to do this project because it has a longer focal length for mammographic energies. Since the output beam is quite small, there was not much scatter generated in any of the measurements.

## B) Contrast Enhancement

The primary benefit of the monochromatizing crystal is increased image contrast. Contrast is defined as

$$C = \ln \left( \frac{I_1}{I_2} \right) \quad (9)$$

where  $I_1$  is the intensity through the area of interest, and  $I_2$  is the adjacent intensity. A phantom to be used at 8 keV has to be relatively thin because there was a lot absorption for regular mammographic phantoms. The phantoms were made of polypropylene plastic, which is easily available from recyclable plastic containers labeled type <5>.

The construction of the phantom is shown in figure 3. The step-height is the difference between the thicknesses of the upper and lower part. The hole pierced in the plastic is for calibrating the direct beam gray scale for different images.

Images were made with each of the three crystals, silicon, mica, and graphite, for the monochromatic case. The detector was a Fuji image plate. The intensity for any area in the image was read with the software.

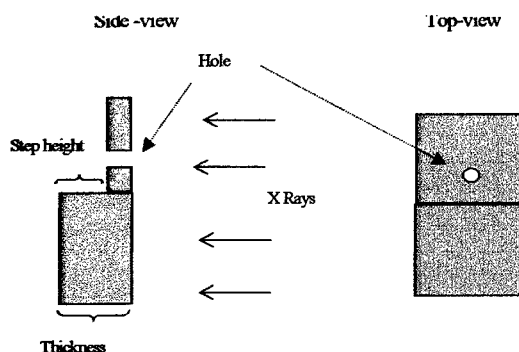


Figure 3. The construction of the 8-keV step phantoms. In the top view the x ray beam is coming straight out of the paper.

is about a factor of five with these phantoms. The improvement factor of five suggests that monochromatic imaging maybe promising when used in clinical settings. Conventional medical imaging can be greatly improved using such a technique. These results also suggest that this work can be developed using higher energies where monochromatic imaging is practiced in clinical settings.

### Objective 5: Design a 20 keV system

In this objective, the candidate learned how to collaborate with a staff from a company for measuring the flux from the molybdenum source.

The theoretical contrast can be calculated from

$$\frac{I_t}{I_o} = e^{-\frac{\mu}{\rho} \rho t} \quad (10)$$

where  $\mu/\rho$  is the mass absorption coefficient for the particular medium,  $\rho$  is the density of the medium, and  $t$  is the thickness of the medium.

For the monochromatic experiment, the expected contrast is calculated directly using equation 9. For the polychromatic case, the actual relative intensity is averaged over 7 - 19 keV.

The contrast ratio is the monochromatic contrast over the polychromatic one. The contrast ratio



Designing a 20 keV system involves an x-ray source, a collimating optic, and a mica crystal since mica provides good contrast and resolution with a high enough intensity. The mica crystal should be thick and firm for easy mounting.

Preliminary testing involves measuring on a test system with silicon because the mica crystals we got were very thin and not easily mountable. With these mica crystals, the flux was lower than expected. For testing at 20 keV, it is sufficient using silicon for gaining a better understanding until we get better mica crystals.

Monochromatic mammographic screening applications should be performed at about 20 keV, so the x-ray energy will not all be absorbed by the patient. Molybdenum tubes are chosen because of the  $K_{\alpha}$  peak at 17.5 keV. The Oxford source with tube voltage of 25 kVp and low power (10 - 20 W) was used to measure the phantoms.

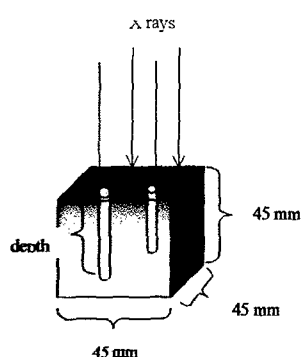


Figure 4. Lucite phantom with different hole depths.

The phantoms for measuring contrast have the same thickness as used in a real mammography system. The construction of Lucite phantom is shown in figure 4. The holes were 3 mm in diameter and the thickness is 45 mm. Each depth was compared without optic and with a combination of optic and crystal at the molybdenum  $K_{\alpha}$  line.

A contrast enhancement of more than a factor of 2 was found experimentally, which agrees well with theoretical calculations. The theoretical contrast was averaged over 8 to 25 keV for the polychromatic case. Table 3 summarizes the results.

The theoretical contrast was calculated the same way as at 8 keV. A quick basic computer program aids in computing theoretical values. After these measurements the source died and needed to be fixed.

Depth (mm)	Polychromatic Contrast		Monochromatic Contrast	
	Data	Theory	Data	Theory
35	$1.3 \pm 0.1$	1.3	$2.4 \pm 0.3$	2.9
30	$1.2 \pm 0.1$	1.0	$2.1 \pm 0.3$	2.5
20	$0.8 \pm 0.1$	0.6	$1.4 \pm 0.4$	1.7
15	$0.4 \pm 0.1$	0.5	$0.7 \pm 0.4$	0.8

Depth (mm)	Contrast Enhancement Ratio:	
	Data	Theory
35	$1.8 \pm 0.6$	2.2
30	$1.8 \pm 0.4$	2.5
20	$2.2 \pm 0.9$	2.8
15	$1.5 \pm 0.9$	1.6

Table 3. Contrast at 17.5 keV with 45-mm Lucite phantom.

Crystals:	Company's specification for $\alpha$ (mrad):	Bragg angle at $K_{\alpha 2}$ 17.3743 keV ( $^{\circ}$ )	$\sigma$ (mrad) with 50- $\mu$ m detector	$\sigma$ (mrad) with an ideal detector	Resultant resolution for 50-mm patient for ideal detector (lp/mm)	Crystal efficiency $\eta$
Silicon	0.02	15.24	0.261	0.201	50	0.005
Mica	0.4-0.6	10.33	0.453	0.421	24	0.10
Graphite	35-87	6.09	4.104	4.101	2	1

Table 4 The theoretical angular resolution using molybdenum  $K_{\alpha 2}$  peak.

The expected resolution at molybdenum  $K_{\alpha}$  peak can be calculated using the same procedure described in objective 3. Assuming,  $K_{\alpha 2}$  peak, which has a width of 7.7 eV, was measured with a 50- $\mu$ m pixel detector, the complete table of the theoretical resolution using silicon, mica, and graphite is given in table 4.

The flux measurements were performed by the source supplier. Shortly, after being brought to our laboratory for the above measurements, the source died.

The flux at 60 kVp and 20 W was  $1.4 \times 10^8$  photons/s.

Theoretically, at 20 W (0.33 mA), the flux is  $2.06 \times 10^8$  photons/sec, which is the same order of magnitude as the experimental one. It seems that the discrepancy is not as large with the molybdenum source as with our rotating anode system.

The Ultra bright molybdenum source gives good preliminary results for the flux calculation as well as the contrast measurements. The thickness of phantoms is more realistic than that at 8 keV. The subject contrast enhancement is a factor of two, in agreement with theoretical calculations. There was no scatter in any of these measurements because the beam was only 10 by 10 mm. With a larger beam, the contrast enhancement would be a factor of two because of the reduction of scattered radiation.

For designing a 20 keV system, the x-ray source should be molybdenum or rhodium because the characteristic lines are at mammographic energies with a thick mica crystal for good flux, contrast, and resolution.

#### **Objective 6: Write a Final Report**

This final report is written and submitted in conclusion to this project.

### **Key Research Accomplishments:**

- The total photon flux from the copper rotating anode source was measured to be  $3.9 \times 10^{10}$  photons/s. The flux from the optic was  $5.1 \times 10^5$  photons/s. The flux from the optic/silicon was 2,000 photons/s, from optic/mica was 4,000 photons/s, and from optic/graphite was 104,000 photons/s.
- The measured angular resolution with a silicon crystal is 0.5 mrad at 8 keV. For a 50-mm thick patient, this angle corresponds to 18 lp/mm. For mica, it is 0.6 mrad at 8 keV which corresponds to 14 lp/mm. For graphite, it is 6.5 mrad at 8 keV, which corresponds to 2 lp/mm.
- The measured angular resolution with a silicon crystal is 0.2 mrad at 17.5 keV. For a 50-mm thick patient, this angle corresponds to 50 lp/mm. For mica, it is 0.4 mrad at 8 keV which corresponds to 24 lp/mm. For graphite, it is 4 mrad at 8 keV, which corresponds to 2 lp/mm.
- Contrast of step height phantoms was enhanced by a factor of 5-6 at 8 keV relative to the conventional polychromatic case.
- Contrast enhancement for a phantom of varying composition was a factor of 6 at 8 keV. These all were in good agreement with the theory.
- At the molybdenum  $K\alpha$  line, 17.5 keV, a contrast enhancement of 2 was measured with a 45-mm thick Lucite phantom, in good agreement with theory.

### **Reportable outcomes**

#### **Publications:**

1. C. A. MacDonald, F. R. Sugiro, and W. M. Gibson, "Improved Radiography with Polycapillary X-Ray Optics, Ali M. Khounsary and C.A. MacDonald, eds., **Advances in Laboratory-Based X-Ray Sources and Optics II**, SPIE vol. 4502, pp. 10-18, 2002.
2. C. A. MacDonald, W. M. Gibson, F. R. Sugiro, "High Contrast Imaging with Polycapillary Optics," **Advances in X-ray Analysis**, 45, Proceedings of the 50<sup>th</sup> Denver X-ray Conference.

#### **Degrees obtained that are supported by this award:**

The candidate received her Pd. D. in physics in May 2002.

**Funding applied for based on work supported by this award:**

The candidate has received a separate post-doctoral training grant to work at the University of Wisconsin at Madison. This post-doctoral funding was made possible because of this pre-doctoral training. She will work in clinical research to apply this work into a real mammography system.

## **Conclusions:**

This final report shows the possibility of a monochromatic imaging with conventional laboratory x-ray sources, which could move this modality to practical clinical mammographic screening. This technique gives high contrast, high resolution, and low patient dose.

Monochromatic imaging was performed using polycapillary optic and a crystal. The crystals were silicon, mica, and graphite. These crystals were chosen because of the availability and the different angular bandwidths. Mica has a large enough bandwidth to give high theoretical photon flux, high enough resolution for mammography, and high contrast.

Resolution would be 24 lp/mm for a 50-mm thick patient. Contrast was better than 2 from a regular molybdenum x-ray source. Since the optic provides a parallel beam, scatter could be reduced by another factor of 2 by extending the distance between the patient and the detector without degrading the image.

This project can be further applied to a clinical training.

**References:**

<sup>1</sup> Mirkin, Lev Iosifovich, Handbook of X-ray Analysis of Polycrystalline Materials.  
Consultants bureau: New York, 1964

<sup>2</sup> Michette A. G. and C. J. Buckley, X-ray Science and Technology, Institute of Physics  
Publishing: Bristol, 1993.